5070

180

TECHNICAL MEMORANDUMS

NATIONAL ADVISORY COMMITTEE FOR AERONAUTICS

No. 983

TEMPERATURE RECORDING IN HIGH-SPEED GASES

By E. Eckert

Zeitschrift des Vereines Deutscher Ingenieure
Vol. 84, No. 43, October 26, 1940

Washington
August 1941

NATIONAL ADVISORY COMMITTEE FOR AERONAUTICS

TECHNICAL MEMORANDUM NO. 983

TEMPERATURE RECORDING IN HIGH-SPEED GASES*

By E. Eckert

Proper temperature recording in flowing gases always requires great care because of the potential errors involved through radiation on the adjacent walls or heat dissipation in the thermometer as a result of the comparatively low heat transfer to the instrument. But these errors become continuously less by ascending gas velocity and can be minimized by the use of appropriate instruments (reference 1). But as soon as high speeds are involved a new difficulty arises; namely, the gas layers immediately adjacent to the thermometer suspended in the flow are slowed down by damming or friction and become heated. Then the instrument records the temperature of these layers rather than the true temperature of the flowing gas which corresponds to the irregular motion of its molecules and would be measured with a thermometer carried along in the flow. But, unfortunately, this is hardly ever attainable in practice. Hence there remains, apart from optical recording methods, only the possibility of securing the true gas temperature from the reading of the stationary thermometer. This requires the knowledge of the temperature rise induced by the deceleration of the gas on the thermometer as obtained by calibration of the instrument in a gas flow of known temperature. The development of suitable thermometer shapes giving the amount of temperature rise if possible without calibration and affording ready repetition, is, however, predicated upon a fundamental elucidation of this heating on a number of elementary body forms.

The theory of similitude applied to the present problem (reference 2) states that the temperature rise ϑ_e experienced by a body when held in a gas flow of speed w - made dimensionless with the temperature rise ϑ_{ad} which the gas experiences by adiabatic damming to speed zero - is a function f of the following constants:

---

*"Temperaturmessung in schnell strömenden Gasen." Z. V D I, vol. 84, no. 43, Oct. 26, 1940, pp. 813-17.

Reynolds number Re, Mach number Ma, equal to the ratio of speed w to sonic velocity, and the Prandtl number Pr, equal to the ratio of the kinematic viscosity to the temperature conductivity of the gas. Hence:

$$\vartheta_e/\vartheta_{ad} = f(\mathrm{Re}, \mathrm{Ma}, \mathrm{Pr})$$

The adiabatic temperature rise ϑ_{ad} is given by equation $\vartheta_{ad} = A\, w^2/2\, g\, c_p$ where g is the acceleration due to gravity; A, the mechanical equivalent of heat; and c_p, the specific heat of gas at constant pressure. For air the temperature rise is, accordingly, 5°, by damming from a speed of 100 meters per second; 20°, by damming from 200 meters per second; and 45°, from 300 meters per second.

PLATE IN LONGITUDINAL FLOW

Laminar Boundary Layer

The plate in longitudinal flow with laminar boundary layer has been treated by Pohlhausen as early as 1921 (reference 3). He computed the temperature field formed on an unheated plate dipped in the flow from Prandtl's boundary layer equations, on the assumption that all material values, inclusive of density, are constant. The result can be reconciled with those from the theory of similitude as relation between temperature ratio $\vartheta_e/\vartheta_{ad}$ and the Prandtl number Pr (curve a, fig. 1). The relationship of the Reynolds and the Mach numbers then becomes evident. For a range of $\mathrm{Pr} = 0.5$ to 2 within which gases are approximately involved, $\vartheta_e/\vartheta_{ad} = \sqrt{\mathrm{Pr}}$ is a very good approximation. For air it amounts to $\mathrm{Pr} = 0.714$ according to the most recent material value determinations; hence $\vartheta_e/\vartheta_{ad} = 0.845$.

The applicability of Pohlhausen's findings has been repeatedly contested ever since its publication because of the assumption of constant density. But a closer analysis gives a picture as follows: The flow outside of the boundary layer is not disturbed by a thin plate; hence the pressure is constant everywhere outside of the boundary layer. Within the boundary layer likewise no appreciable pressure differences can be built up. Thus, a change in the density on the plate results only from the temperature rise in the boundary layer as a result of internal friction and this is not very great up to Mach numbers of about 1, so that in this range the Pohlhausen solution should be correct. A further check is possible for a gas with $Pr = 1$, for which the rigorous theoretical calculation even with allowance for the variability of the material values is available. It was originally given by Busemann (reference 4). According to it, the effect of the variability of the material values on the temperature rise in the boundary layer is very insignificant up to a Mach number of $Ma = 2$ (reference 5). The same must hold for gases, whose Pr number does not differ much from 1, hence for air also.

Results of test at subsonic velocity.- As a check on the described theoretical results several experiments were made with thermocouples of 0.1 to 0.5 millimeter diameter (reference 6) butt-soldered together and with 5-millimeter φ brass tubes housed in a nozzle, as shown in figure 2. The temperature was tapped at from a few millimeters to 2 centimeters from the tip. As long as the boundary layer thickness remains small compared to diameter, the problem is exactly the same as on the plate. The experiments were made in air. As indicated by figure 3, the ratio $\vartheta_e/\vartheta_{ad}$ is almost unaffected by the air speed w, the distance of the junction from the nozzle tip and of the wire gage, that is, independent of Re and Ma, amounting to 0.85 for air, against Pohlhausen's $\vartheta_e/\vartheta_{ad} = 0.845$. The agreement between theory and test is therefore very satisfactory. The slight rise in the temperature ratio at high speed is probably attributable to incipient turbulence in the boundary layer.

Results of tests at supersonic speed.- An extension of our test data to include $Ma > 1$ represents measurements made by Nusselt back in 1916 with thermocouples of 0.5 mm φ in a Laval nozzle (reference 7). Nusselt's own conclusion was that a temperature measurement with thermocouples is impossible at high air speeds. But if the measurements are so interpreted that $\vartheta_e/\vartheta_{ad}$ is afforded, it yields the value 0.85 at one thermocouple and 0.84 on a second, and with very little scatter for Mach numbers between 1.7 and 2.2. Those at lower Ma do not lend themselves to evaluation because the flow is then disturbed by compression shocks. So these measurements are also in good agreement with theory.

Turbulent Boundary Layer

The laminar boundary layer develops, as is known, only on the plate leading edge and changes at a certain distance from it to turbulent. From measurements at slow speeds it is known that by undisturbed inflow the Reynolds number, formed with the distance from the plate leading edge, is 500,000. Applied to air at sonic velocity, it means a distance of 2 centimeters of the transition point from the plate leading edge, provided that at this high speed the critical Reynolds number still has the same magnitude. To gain an insight into the temperature rise in the turbulent boundary layer, the 5-millimeter φ tube was pulled out farther from the nozzle, bringing the point where the temperature was tapped up to 85 millimeters away from the nozzle. Figure 4 shows $\vartheta_e/\vartheta_{ad}$ in relation to the Re formed with the distance from the nozzle tip. The turbulent boundary layer manifests a temperature rise, which, however, is not very great.

Pitot Tube Thermometer

According to the foregoing the plate is practical as a temperature-recording instrument if care is taken that the measurement is effected in the laminar boundary layer. The design of the instrument itself depends upon the test purposes. For subsonic speed tests we developed a pitot-tube thermometer which in its outside shape resembled a pitot. The instrument is constructed of thin-walled steel pipe a of 0.2 millimeter thickness, to prevent errors through heat transfer. The junction b for the thermocouple is slightly back of the tip. The instrument was designed in dimensions of from 2 to 6 millimeters φ and calibrated in straight nozzles and in a high-speed tunnel. In all cases the recorded $\vartheta_e/\vartheta_{ad}$ agreed very closely with Pohlhausen's data. Figure 6 gives the calibration curve of such an instrument with 6 millimeters φ. The slight temperature rise indicated in figure 6 at higher speeds is probable to a slight turbulence.

CYLINDER IN TRANSVERSE FLOW

Cylinder of Good Heat-Conducting Material

In order to gain an insight into the conditions accompanying transversely mounted instruments the specific temperature of cylinders in transverse flow will be analyzed. Figure 7 gives the ratio $\vartheta_e/\vartheta_{ad}$ for transversely mounted cylinders of different diameters plotted against the Mach number (reference 7). The cylinders being of good heat-conducting material, no temperature difference occurred within one section. The curves a, b, and c, were plotted at different gas temperatures. Two unusual facts are evident: first, the values $\vartheta_e/\vartheta_{ad}$ are partly located very low; secondly, the profound dependence on the Mach number, i.e., on the speed. The lowest $\vartheta_e/\vartheta_{ad}$, which lies at about Ma = 0.6, corresponds to air speed at which velocity of sound is precisely reached on the side of the cylinder. So, because of the marked variation of $\vartheta_e/\vartheta_{ad}$, transversely mounted thermometers are unsuitable for recording temperatures at high speeds.

Cylinder of Poor Heat-Conducting Material

With a view to gaining further insight into the conditions surrounding cylinders in the transverse flow the local specific temperatures were measured across the circumference of hard rubber cylinders of 10 and 20 millimeters φ (reference 6). The results for a Mach number of $Ma_o = 0.685$ formed with the air speed are illustrated in figure 8. Curve b manifests over half of the circumference the aspect of the static pressure p measured through a fine hole in the cylinder, curve c the ratio $\vartheta_e/\vartheta_{ad}$, where ϑ_{ad_o} is the temperature rise corresponding to the damming from the flow velocity and ϑ_{e_o} the temperature difference between cylinder surface and air in inflow condition. The stagnation temperature is reached on the forward stagnation point, and with increasing α the temperature of the cylinder surface drops in proportion to the rising speed. If the local specific temperature is referred to the adiabatic temperature rise ϑ_{ad} associated with the local speed w, curve d is afforded, which, as far as the separation point, has the same magnitude as the flat plate (fig. 3). Unusual, on the other hand, is the low temperature behind junction B at around 80°, which in part is even lower than the true temperature of the flowing gas. This is possible of itself, because the gas, on flowing past the cylinder, has at the point where the pressure curve indicates negative values a higher speed and therefore a lower temperature than in the inflow.

Even so it is surprising that the air, which lost so much of its speed in the dead-air region, did not heat up to stagnation temperature by conversion of motion into thermal energy.

STAGNATION TEMPERATURE RECORDING

Spherical Thermometer

The conclusions that can be drawn from figure 8 are as follows: first, the use of transversely mounted thermometers in temperature recording is not recommended because of the great temperature differences over the circumference; secondly, it must be possible of itself to design an instrument, patterned perhaps after a Prandtl pitot tube, which also records the stagnation temperature at the stagnation point when the instrumet is of corresponding size and made of poor heat-conducting material so as to hold down the heat transfer in the instrument from the stagnation point where high speeds and hence low temperatures prevail. For this reason Wimmer located the thermocouple junction of his spherical thermometer (reference 8) slightly before the sphere surface (fig. 9). This is above all dictated by the good heat-conducting material of the sphere. The calibration curve (fig. 10) is very satisfactory. Admittedly, the given dimensions must be very accurately maintained. Therefore no reduction of the sphere for local temperature measurements is possible. And the vulnerability of the freely exposed thermocouple in service measurements is also somewhat disturbing.

Diffuser Thermometer

Another possibility of recording temperatures closely approaching stagnation temperature is afforded by Franz's diffuser instrument (reference 9). A slightly modified version of 6-millimeters diameter is shown in figure 11; the related calibration curve in figure 12. The damming of the air is dealt with in the diffuser. Because of the continuous escape of a little air through the side openings the dammed air is prevented from cooling through heat transfer on the walls and so causes wrong measurements.

The last two described instruments which record the stagnation temperature with sufficient accuracy have the advantage of precluding any increase in the reading due to turbulence; hence they are practical for measuring in very turbulent gas flows. The pitot thermometer itself has in its favor simplicity of design, diversity of size, and absence of errors due to heat transfer.

RELATION OF ANGLE TO THERMOMETER READING

Another important fact in the appraisal of a temperature-recording instrument is the relation of its indication to the direction of flow, and it is particularly desirable that the indication not change if the instrument is slightly tilted. The relationship of temperature ratio $\vartheta_e / \vartheta_{ad}$ to the inclination of the instrument in the flow direction for the pitot thermometer is shown in figure 13. The reading is constant within -10° to $+10^\circ$ angle. It is approximately the same range within which the reading of the velocity pressure of a Prandtl pitot remains unchanged. The same holds true for the spherical thermometer (reference 8) and for the diffuser thermometer which had been explored also for angular relationship. In this respect the three instruments are therefore equivalent.

Translation by J. Vanier,
National Advisory Committee
for Aeronautics.

REFERENCES

1. VDI Temperaturmessregeln. (Berlin) 1940.

2. Weber, M.: Das Ähnlichkeitsprinzip der Physik und seine Bedeutung für das Modellversuchswesen, Forsch. Ing.-Wes., vol. 11, no. 2, 1940, pp. 49-58.

3. Pohlhausen, E.: Z.f.a.M.M., vol. 1, 1921, pp. 115-21.

4. Busemann, A.: Z.f.a.M.M., vol. 15, 1935, pp. 23-25.

5. Eckert, E., and Drewitz, O.: Forsch. Ing.-Wes, vol. 11, no. 3, 1940, pp. 116-24.

6. Über die Messungen selbst wird in Forsch. Ing.-Wes. vol. 12, no. 1, 1941 eingehender berichtet.

7. Nusselt, W.: Z. ges. Turbinenwes. vol. 13, 1916, p. 172.

8. Wimmer, W.: Stagnation Temperature Recording. T.M. No. 967, NACA, 1941.

9. Franz, A.: Pressure and Temperature Measurement in Supercharger Investigations. T.M. No. 953, NACA, 1940.

FIGURE LEGENDS

Figure 1.- Temperature rise ϑ_e of unheated plate in high-speed flow with laminar boundary layer
ϑ_{ad} temperature rise by adiabatic damming
Curve a is the result of the exact calculation according to Pohlhausen

Figure 2.- Cylinder in non-enlarged nozzle b
T_e temperature of cylinder at test station
T_o temperature in gas flow of speed w
T_k temperature in tank before nozzle

Figure 3.- Recorded temperature rise $\vartheta_e = T_e - T_o$ of unheated cylinder a of fig. 2 in flow with laminar boundary layer
$\vartheta_{ad} = T_k - T_o$ temperature rise by adiabatic damming

Figure 4.- Temperature rise ϑ_e of cylinder with laminar and turbulent boundary layer flow
ϑ_{ad} temperature rise by adiabatic damming

Figure 5.- Pitot thermometer
a nickel-plated iron tube, 6-mm φ, 0.2 mm-wall thickness
b temperature tap: copper block soldered in iron tube
c 0.5-mm φ constantan-manganese thermocouple
w flow velocity

Figure 6.- Calibration curve of instrument of fig. 5
ϑ_{ad} temperature rise by adiabatic damming
ϑ_e temperature rise of thermometers

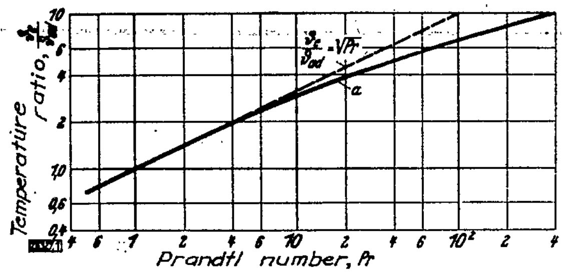

Figure 1.

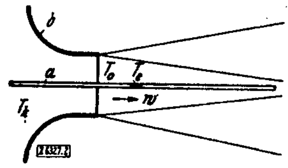

Figure 2.

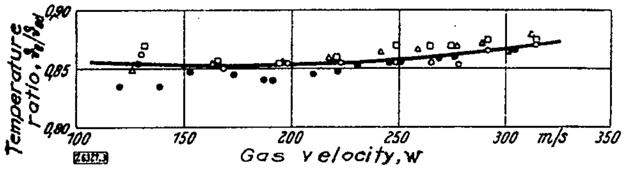

Figure 3.

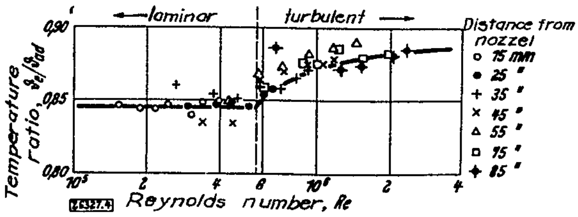

Figure 4.

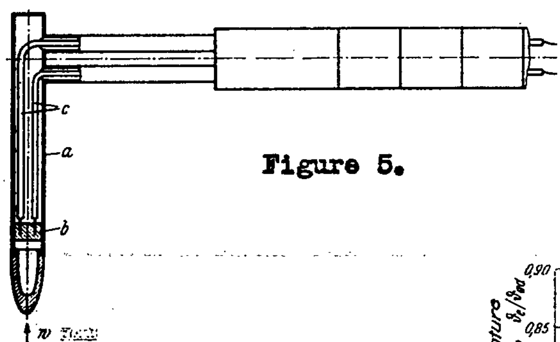

Figure 5.

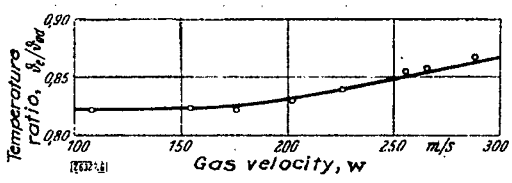

Figure 6.

Figure 7.- Temperature rise ϑ_e in transverse flow of cylinders of good heat-conducting material with different diameters d
Curve a was recorded at 19° temperature in gas flow,
Curve b at 15° tank temperature,
Curve c at 50° tank temperature

Figure 8.- Pressure and temperature distribution over the circumference of a transversely exposed cylinder of d diameter made of poor heat-conducting material
Air speed: w_o = 227 m/s, $Ma_o = w_o/a = 0.685$, $Re_o = w_o d/\nu = 1.4 \times 10^5$
p, T_e pressure and temperature on surface at angle α to stagnation point
T_o, w_o temperature and speed in undisturbed air stream
T, w temperature and speed outside of boundary layer at point of circumference defined by angle α
A mechanical equivalent of heat
a velocity of sound
ν kinematic viscosity
c_p specific heat
g gravity
Pressure distribution curve b indicates the place where locally sonic velocity is reached ($Ma = w/a = 1$) and where the maximum local Mach number occurs ($Ma = w/a = 1.08$)

Figure 9.- Spherical thermometer
a 10 mm φ steel sphere
b plastic cylinder
c 0.5 mm φ iron-constantan thermocouple

Figure 10.- Calibration curve for fig. 9

Figure 11.- Diffusor-thermometer
a 6 mm φ nickel-plated steel tube, 0.2 mm wall thickness
b diffusor
c discharge openings
d 0.5-mm constantan-manganese thermocouple
e glass tube
f hard rubber cylinder

Figure 12.- Calibration curve for fig. 11

Figure 13.- Relation of angle α to pitot-thermometer reading

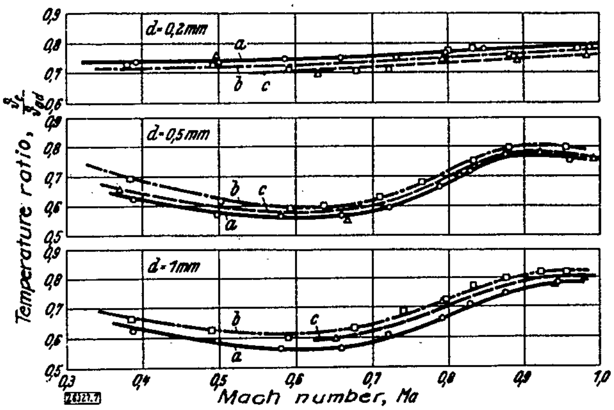

Figure 7.

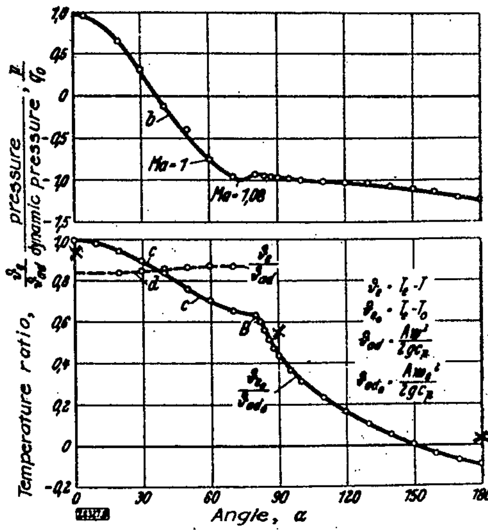

NOTES:
VEL. APPROX 523 M.P.H
× POINTS ARE ESTIMATED FROM HILTONS

Figure 8.

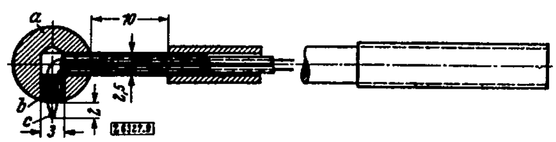

Figure 9.

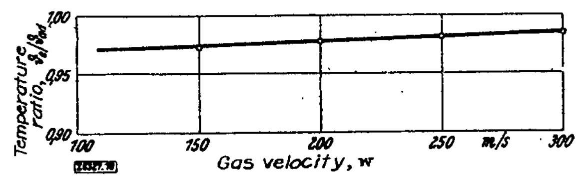

Figure 10.

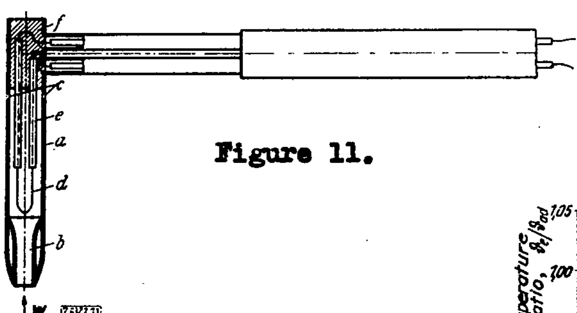

Figure 11.

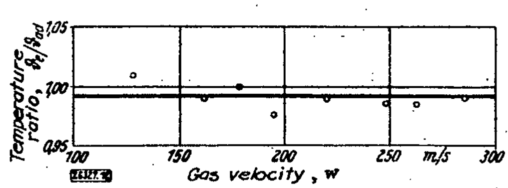

Figure 12.

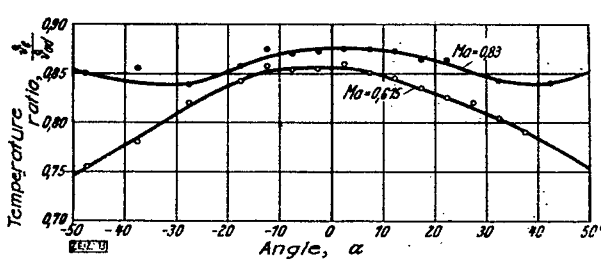

Figure 13.